Phase Locked Loop (PLL):

$$V_{sa}(t) = \widehat{V}_s \cos(\omega_0 t + \theta_0),$$
$$V_{sb}(t) = \widehat{V}_s \cos\left(\omega_0 t + \theta_0 - \frac{2\pi}{3}\right),$$
$$V_{sc}(t) = \widehat{V}_s \cos\left(\omega_0 t + \theta_0 - \frac{4\pi}{3}\right),$$

$$\vec{V}_s(t) = \widehat{V}_s e^{j(\omega_0 t + \theta_0)}. \qquad f_d + jf_q = \vec{f}\,(t) e^{-j\rho(t)}$$

$$V_{sd} = \widehat{V}_s \cos(\omega_0 t + \theta_0 - \rho),$$
$$V_{sq} = \widehat{V}_s \sin(\omega_0 t + \theta_0 - \rho).$$

ρ(t) = ωot + θo corresponds to Vsq = 0. Therefore, we devise a mechanism to regulate Vsq at zero.

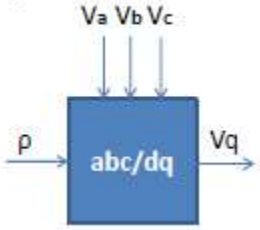

This can be achieved based on the following feedback law:

$$\omega(t) = H(p) V_{sq}(t)$$

linear transfer function (compensator)

$$p = d(\cdot)/dt$$

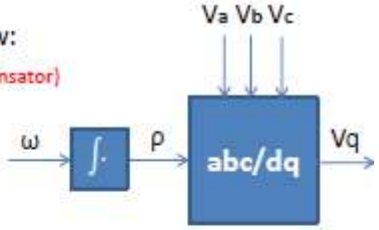

$$\left.\begin{aligned} V_{sq} &= \widehat{V}_s \sin(\omega_0 t + \theta_0 - \rho) \\ \frac{d\rho}{dt} &= \omega(t) \end{aligned}\right\} \longrightarrow \underbrace{\frac{d\rho}{dt} = H(p)\widehat{V}_s \sin(\omega_0 t + \theta_0 - \rho)}$$

This equation describes a nonlinear dynamic system, which is referred to as PLL

The function of the PLL is to regulate ρ at ωot + θo. However, in view of its nonlinear characteristic, the PLL can exhibit unsatisfactory behavior under certain conditions. For example, if the PLL starts from an initial condition corresponding to ρ(0) = 0 and ω(0) = 0, then the term Vs^H(p) sin(ωot + θo − ρ) is a sinusoidal function of time with frequency ωo. Then, if H(s) has a low-pass frequency response, the right-hand side and also dρ/dt exhibit small sinusoidal perturbations about zero, the PLL falls in a limit cycle, and ρ does not track ωot + θo.

To prevent the limit cycle from taking place, the control law can be modified as:

$$\omega(t) = H(p)V_{sq}(t), \quad \omega(0) = \omega_0 \text{ and } \omega_{min} \le \omega \le \omega_{max}$$

ω(t) has the initial value ω(0) = ωo and is limited to the lower and upper limits.

1) ωmin and ωmax are selected to be close to ωo and thus to define a narrow range of variations for ω(t).
2) On the other hand, the range of variations should be selected adequately wide to permit excursions of ω(t) during transients.

If the PLL tracks ωot + θo, the term ωot + θo − ρ is close to zero and
sin(ωot + θo − ρ) ≈ (ωot + θo − ρ).

Therefore: $$\frac{d\rho}{dt} = \hat{V}_s H(p)(\omega_0 t + \theta_0 - \rho)$$

This represents a classical feedback control loop in which ωot + θo is the reference input, ρ is the output, and Vs^H(s) is the transfer function of the effective compensator

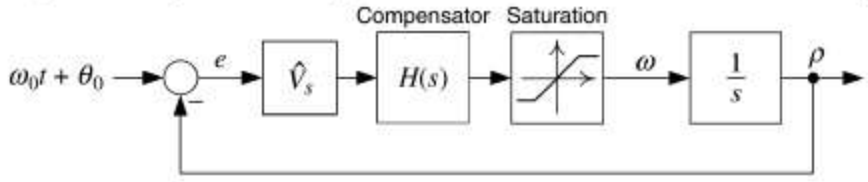

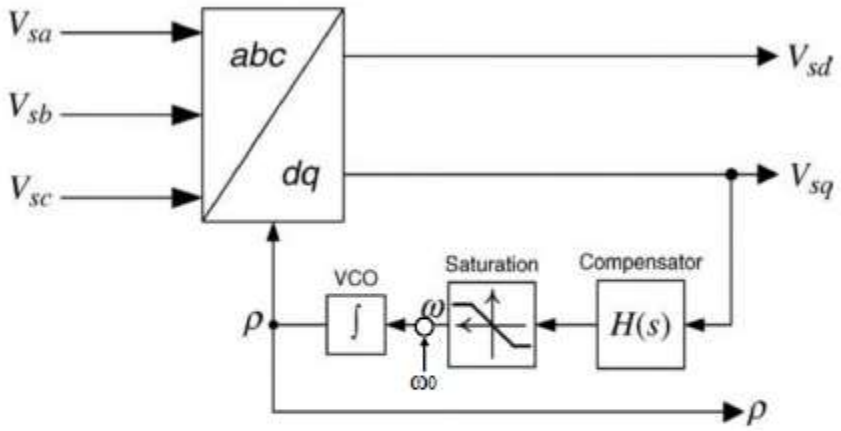

the integrator is realized by means of a voltage-controlled oscillator (VCO). The VCO can be regarded as a resettable integrator whose output, ρ, is reset to zero whenever it reaches 2π.

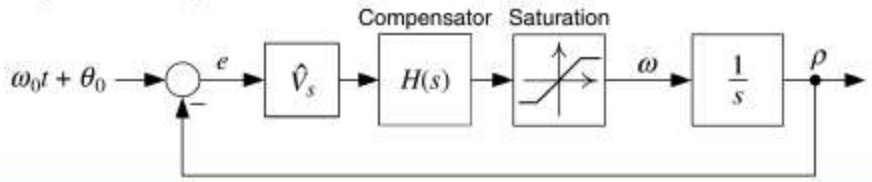

the reference signal, ωot + θo, is composed of two components:

1) a constant component, that is, θo

Since the loop gain includes an integral term, ρ tracks the constant component of the reference signal with zero steady-state error.

2) a ramp function, that is, ωot.

To ensure a zero steady-state error for the ramp component, the loop gain must include at least two integrators.

Therefore, $H(s)$ must include at least one integral term, that is, one pole at $s = 0$. The other poles and zeros of $H(s)$ are determined mainly on the basis of the closed-loop bandwidth of the PLL and stability indices such as phase margin and gain margin.

Assume that V_{sabc} represents an unbalanced voltage with a negative-sequence fundamental component and a fifth-order harmonic component ,as

$$V_{sa}(t) = \overbrace{\left\{\hat{V}_s \cos(\omega_0 t + \theta_0)\right\}}^{V_{1abc}} + \overbrace{\left\{k_1 \hat{V}_s \cos(\omega_0 t + \theta_0)\right\}}^{V_{1acb}} + \overbrace{\left\{k_5 \hat{V}_s \cos(5\omega_0 t + \phi_5)\right\}}^{V_{5abc}}$$

$$V_{sb}(t) = \overbrace{\left\{\hat{V}_s \cos\left(\omega_0 t + \theta_0 - \frac{2\pi}{3}\right)\right\}}^{V_{1abc}} + \overbrace{\left\{k_1 \hat{V}_s \cos\left(\omega_0 t + \theta_0 - \frac{4\pi}{3}\right)\right\}}^{V_{1acb}} + \overbrace{\left\{k_5 \hat{V}_s \cos\left(5\omega_0 t + \phi_5 - \frac{4\pi}{3}\right)\right\}}^{V_{5abc}}$$

$$V_{sc}(t) = \overbrace{\left\{\hat{V}_s \cos\left(\omega_0 t + \theta_0 - \frac{4\pi}{3}\right)\right\}}^{V_{1abc}} + \overbrace{\left\{k_1 \hat{V}_s \cos\left(\omega_0 t + \theta_0 - \frac{2\pi}{3}\right)\right\}}^{V_{1acb}} + \overbrace{\left\{k_5 \hat{V}_s \cos\left(5\omega_0 t + \phi_5 - \frac{2\pi}{3}\right)\right\}}^{V_{5abc}}$$

k1 and k5 are the amplitudes of the negative-sequence (fundamental) and fifth-order harmonic components, respectively, relative to the amplitude of the positive-sequence (fundamental) component.

Typically values of k1 and k5 are assumed to be 0.01 and 0.025, respectively. However, under single-phase to ground faults, k1 can be as large as 0.5.

the space phasor corresponding to V_{sabc} is:

$$\vec{V}_s = \hat{V}_s e^{j(\omega_0 t+\theta_0)} + k_1 \hat{V}_s e^{-j(\omega_0 t+\theta_0)} + k_5 \hat{V}_s e^{-j(5\omega_0 t+\phi_5)}.$$

If the PLL is under a steady-state operating condition, that is, $\rho = \omega_0 t + \theta_0$, then

$f_d + jf_q = \vec{f}(t)e^{-j\rho(t)}$

$$\begin{cases} V_{sd} = \hat{V}_s + k_1 \hat{V}_s \cos(2\omega_0 t + 2\theta_0) + k_5 \hat{V}_s \cos(6\omega_0 t + \theta_0 + \phi_5), \\ V_{sq} = -k_1 \hat{V}_s \sin(2\omega_0 t + 2\theta_0) - k_5 \hat{V}_s \sin(6\omega_0 t + \theta_0 + \phi_5). \end{cases}$$

In addition to DC components, V_{sd} and V_{sq} include sinusoidal components with frequencies $2\omega_0$ and $6\omega_0$.

Between the two AC components of V_{sq}, the component with frequency $2\omega_0$ is more important. The reason is that (i) the frequency of this component is three times lower than that of the other component and (ii) the magnitude of this component, k1, can be significantly larger than that of the other component, for example, during a fault.

One approach to attenuate the double-frequency component of V_{sq} is to ensure that H(s) exhibits a strong low-pass characteristic. However, this method may compromise the PLL closed-loop bandwidth. Alternatively, one can include in H(s) one pair of complex-conjugate zeros, at $s = \pm j2\omega_0$, to eliminate the double-frequency ripple of V_{sq}. The advantage of this technique is that the PLL closed-loop bandwidth is not sacrificed and can be selected to be arbitrarily large.

Consider the PLL of Fig. page 230 whose input is V_{sabc} defined by Eq. 232 where $\omega_0 = 2\pi \times 60$ rad/s and $\hat{V}_s = 391$ V. The objective is to design the PLL compensator $H(s)$.

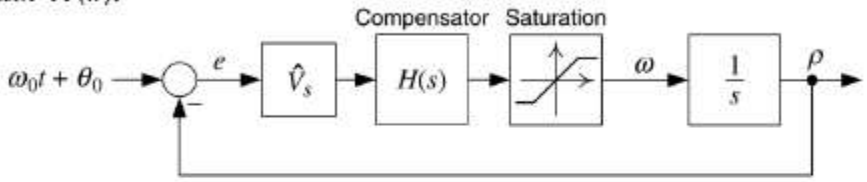

As explained before, $H(s)$ must include one pole at $s = 0$ and the complex-conjugate zeros $s = \pm j2\omega_0$. In addition, to ensure that the loop gain magnitude continues to drop with the slope of -40 dB/dec for $\omega > 2\omega_0$, a double real pole at $s = -2\omega_0$ is included in $H(s)$. Thus,

$$H(s) = \left(\frac{h}{\hat{V}_{sn}}\right) \frac{s^2 + (2\omega_0)^2}{s(s + 2\omega_0)^2} F(s),$$

H(s) is normalized such that the constant gain of the loop gain h is independent of $\hat{V}_{sn}$.

where $\hat{V}_{sn}$ is the nominal value of $\hat{V}_s$ and $F(s)$ is the proper transfer function with no zero at $s = 0$.

Based on the block diagram of Figure , the loop gain is formulated as

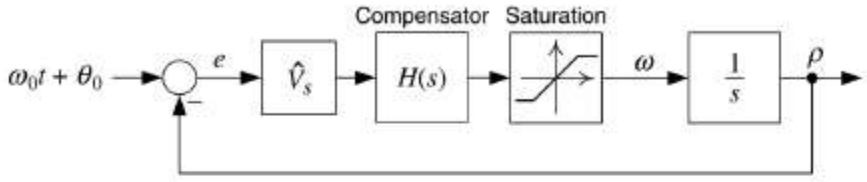

$$\ell(s) = h\frac{s^2 + (2\omega_0)^2}{s^2(s + 2\omega_0)^2}F(s).$$

Let us assume that we need a gain crossover frequency of $\omega_c = 200$ rad/s and a phase margin of 60°. If $hF(s) = 1$, it can be calculated that $\angle\ell(j200) = -210°$. Thus, to achieve the required phase margin, $F(j200)$ must add 90° to $\angle\ell(j200)$. As discussed before , a lead compensator can offer an optimum phase advance to the loop gain. In this example, the required phase advance is fairly large. Consequently, $F(s)$ can be composed of two cascaded lead compensators, each to provide 45° at 200 rad/s. Thus,

$$F(s) = \left(\frac{s + (p/\alpha)}{s + p}\right)\left(\frac{s + (p/\alpha)}{s + p}\right), \qquad p = \omega_c\sqrt{\alpha}$$

$$\alpha = \frac{1 + \sin\delta_m}{1 - \sin\delta_m},$$

δ_m is the phase of each lead compensator at ω_c. If $\delta_m = 45°$

$$F(s) = \left(\frac{s + 83}{s + 482}\right)^2.$$

$$\ell(s) = \frac{h\left(s^2 + 568{,}516\right)\left(s^2 + 166s + 6889\right)}{s^2\left(s^2 + 1508s + 568{,}516\right)\left(s^2 + 964s + 232{,}324\right)}.$$

then follows from $|\ell(j200)| = 1$ and $\widehat{V}_{sn} = 391$ V that $h = 2.68 \times 10^5$. Therefore, $h/\widehat{V}_{sn} = 685.42$ and the final compensator is

$$H(s) = \frac{685.42\left(s^2 + 568{,}516\right)\left(s^2 + 166s + 6889\right)}{s\left(s^2 + 1508s + 568{,}516\right)\left(s^2 + 964s + 232{,}324\right)} \quad [(\text{rad/s})/\text{V}].$$

frequency response

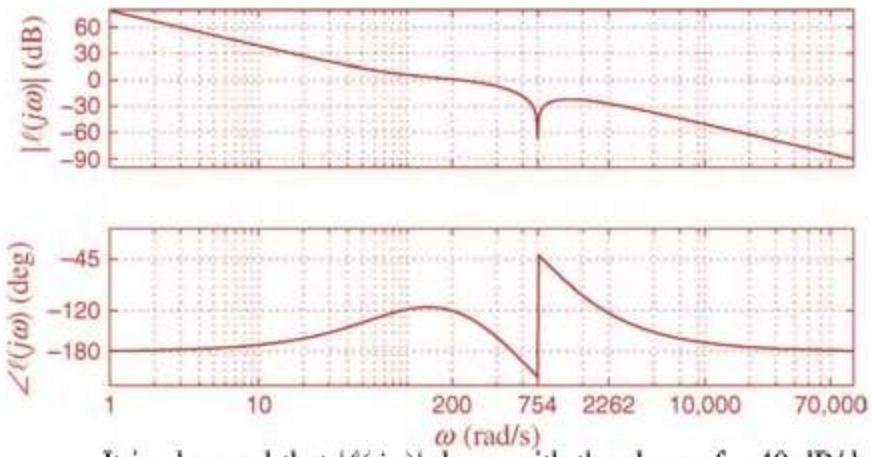

It is observed that $|\ell(j\omega)|$ drops with the slope of -40 dB/dec, for $\omega \ll \omega_c = 200$. However, around ω_c the slope of $|\ell(j\omega)|$ reduces to about -20 dB/dec and $\angle\ell(j\omega)$ rises to about -120° at $\omega = \omega_c$, corresponding to a phase margin of 60°. Figure 8.6 also illustrates that $|\ell(j\omega)|$ continues to drop with a slope of -40 dB/dec for $\omega > \omega_c$. This characteristic is desired as the AC components of V_{sq} due to the harmonic distortion of V_{sabc} are attenuated. In particular, at $\omega = 6\omega_0$, $|\ell(j\omega)|$ is about -30 dB.

Figure shows that, from t=0 to t=0.07s, the compensator output is saturated at $\omega_{min}=2\pi\times55$rad/s, therefore, V_{sd} and V_{sq} vary with time. At about t=0.07s, V_{sq} crosses zero and intends to become negative. Thus, H(s) increases ω to regulate V_{sq} at zero. Figure indicates that V_{sq} is regulated at zero within 0.15 s. It should be noted that if ω_{min} is selected closer to ω_0, the start-up transient period becomes shorter. However, ω_{min} cannot be selected too close to ω_0 since the PLL would not be able to quickly react to other types of disturbance.

Start-up response of the PLL

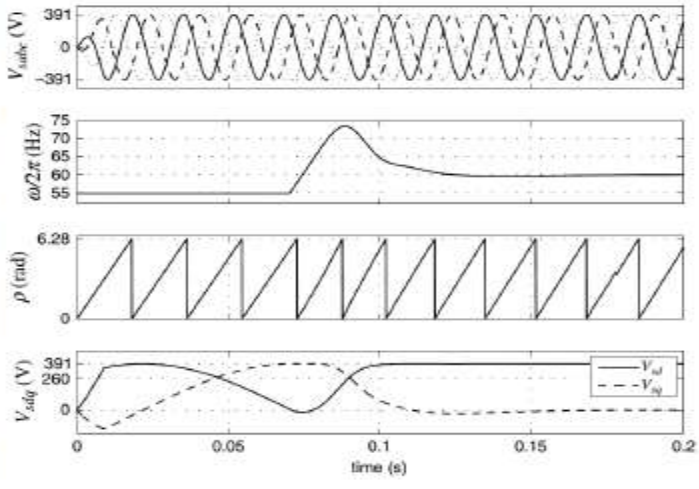

Figure illustrates the dynamic response of the PLL to a sudden imbalance in V_{sabc}. Initially, the PLL is in a steady state. At t=0.05s, the AC system voltage Vsabc becomes unbalanced such that V^s and k1 undergo step changes, respectively, from 391 to 260 V and from zero to 0.5, and at t=0.15 s, V_{sabc} reverts to its balanced predisturbance condition. In response to the voltage imbalance, H(s) transiently changes ω, as Figure shows, to maintain the DC component of V_{sq} at zero. Figure also shows that V_{sq} (and V_{sd}) includes a 120-Hz sinusoidal ripple due to the negative-sequence component of V_{sabc}. The ripple is, however, suppressed by H(s), and ω and ρ remain free of distortion.

Response of the PLL to a sudden AC system voltage imbalance

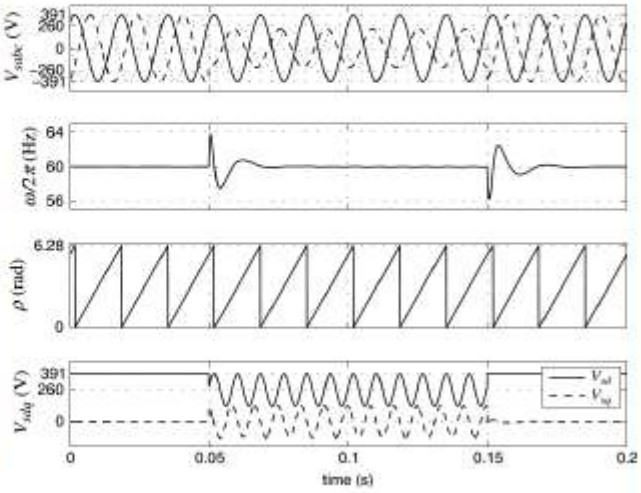

Figure depicts the dynamic response of the PLL to two stepwise changes in ω_0, the first one from $2\pi\times60=377$rad/s to $2\pi\times63=396$rad/s at t=0.05s, and the other from 396 rad/s to $2\pi\times57=358$rad/s at t=0.1s. As Figure shows, V_{sq} is rapidly regulated at zero and ω tracks the changes.

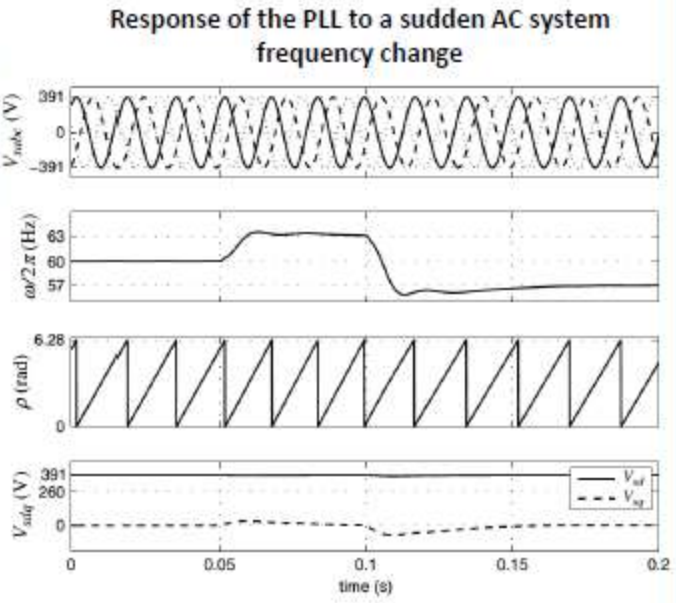

$$\begin{cases} P_s(t) = \frac{3}{2}\left[V_{sd}(t)i_d(t) + V_{sq}(t)i_q(t)\right], \\ Q_s(t) = \frac{3}{2}\left[-V_{sd}(t)i_q(t) + V_{sq}(t)i_d(t)\right], \end{cases}$$

if the PLL is in a steady state, $V_{sq}=0$

$$\begin{cases} P_s(t) = \frac{3}{2}V_{sd}(t)i_d(t), \\ Q_s(t) = -\frac{3}{2}V_{sd}(t)i_q(t). \end{cases}$$

Therefore, $P_s(t)$ and $Q_s(t)$ can be controlled by i_d and i_q, respectively. Let us introduce

$$i_{dref}(t) = \frac{2}{3V_{sd}}P_{sref}(t),$$

$$i_{qref}(t) = -\frac{2}{3V_{sd}}Q_{sref}(t).$$

Then, if the control system can provide fast reference tracking, that is, $i_d \approx i_{dref}$ and $i_q \approx i_{qref}$, then $P_s \approx P_{sref}$ and $Q_s \approx Q_{sref}$, that is, $P_s(t)$ and $Q_s(t)$, can be independently controlled by their respective reference commands. Since V_{sd} is a DC variable (in the steady state), i_{dref} and i_{qref} are also DC variables if P_{sref} and Q_{sref} are constant signals. Thus, as expected, the control system in dq-frame deals with DC variables, unlike the control system in $\alpha\beta$-frame that deals with sinusoidal signals.

VSC Current Control:

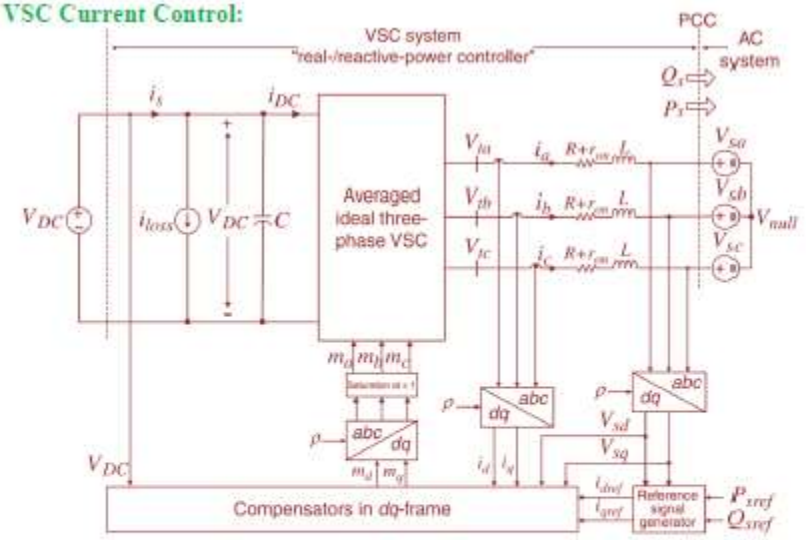

$$L\frac{di_d}{dt} = L\omega_0 i_q - (R + r_{on})i_d + V_{td} - V_{sd}, \qquad V_{td}(t) = \frac{V_{DC}}{2}m_d(t),$$

$$L\frac{di_q}{dt} = -L\omega_0 i_d - (R + r_{on})i_q + V_{tq} - V_{sq}, \qquad V_{tq}(t) = \frac{V_{DC}}{2}m_q(t).$$

id , iq: state variables Vtd , Vtq: control inputs Vsd , Vsq: disturbance inputs

VSC Current Control:

$$L\frac{di_d}{dt} = L\omega_0 i_q - (R + r_{on})i_d + V_{td} - V_{sd},$$

$$L\frac{di_q}{dt} = -L\omega_0 i_d - (R + r_{on})i_q + V_{tq} - V_{sq},$$

Due to the presence of $L\omega_0$ terms, dynamics of id and iq are coupled. To decouple the dynamics, we determine m_d and m_q as:

$$m_d = \frac{2}{V_{DC}}\left(u_d - L\omega_0 i_q + V_{sd}\right),$$

$$m_q = \frac{2}{V_{DC}}\left(u_q + L\omega_0 i_d + V_{sq}\right),$$

feed-forwards

where u_d and u_q are two new control inputs.

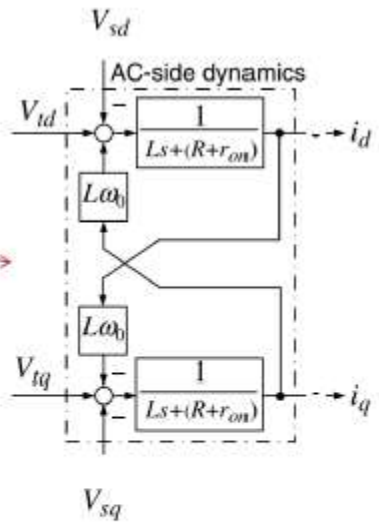

then:

$$L\frac{di_d}{dt} = -(R + r_{on})i_d + u_d,$$

$$L\frac{di_q}{dt} = -(R + r_{on})i_q + u_q.$$

two decoupled, first-order, linear systems.

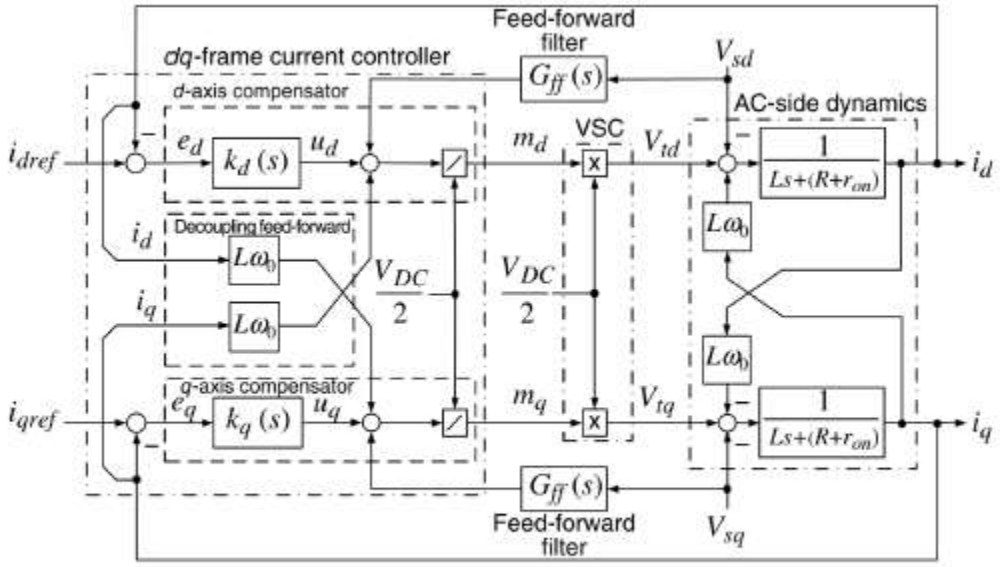
Feed-forward filter
dq-frame current controller
$G_{ff}(s)$
V_{sd}
d-axis compensator
AC-side dynamics
i_{dref}
e_d
$k_d(s)$
u_d
m_d
VSC
V_{td}
$\frac{1}{Ls+(R+r_{on})}$
i_d
Decoupling feed-forward
$L\omega_0$
i_d
i_q
$\frac{V_{DC}}{2}$
q-axis compensator
i_{qref}
e_q
$k_q(s)$
u_q
m_q
V_{tq}
i_q
$G_{ff}(s)$
Feed-forward filter
V_{sq}

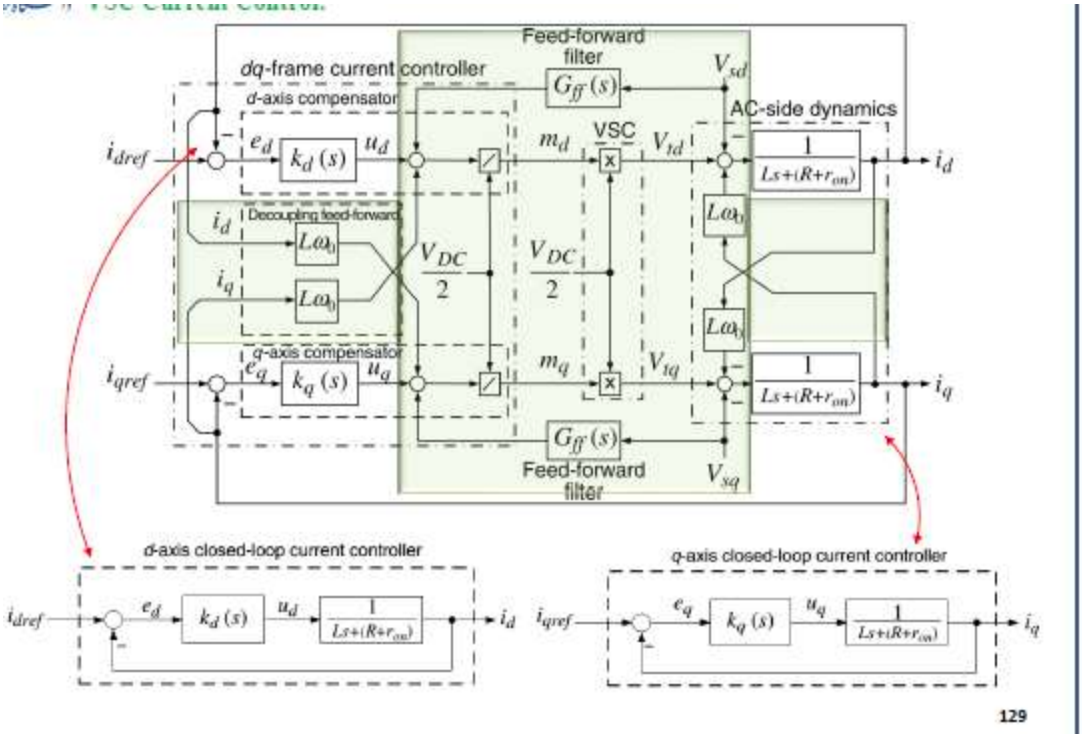
Feed-forward filter
dq-frame current controller
$G_{ff}(s)$
V_{sd}
d-axis compensator
AC-side dynamics
i_{dref}
e_d
$k_d(s)$
u_d
m_d
VSC
V_{td}
$\frac{1}{Ls+(R+r_{on})}$
i_d
Decoupling feed-forward
$L\omega_0$
i_d
i_q
$\frac{V_{DC}}{2}$
q-axis compensator
i_{qref}
e_q
$k_q(s)$
u_q
m_q
V_{tq}
i_q
$G_{ff}(s)$
Feed-forward filter
V_{sq}
d-axis closed-loop current controller
q-axis closed-loop current controller

Unlike the αβ-frame control where the compensators are fairly difficult to optimize and typically are of high dynamic orders, $k_d(s)=k_q(s)$ can be a simple proportional-integral (PI) compensator to enable tracking of a DC reference command.

$$k_d(s) = \frac{k_p s + k_i}{s}, \quad \longrightarrow \quad \ell(s) = \left(\frac{k_p}{Ls}\right) \frac{s + k_i/k_p}{s + (R + r_{on})/L}.$$

It is noted that due to the plant pole at $s = -(R + r_{on})/L$, which is fairly close to the origin, the magnitude and the phase of the loop gain start to drop from a relatively low frequency. Thus, the plant pole is first canceled by the compensator zero $s = -k_i/k_p$, and the loop gain assumes the form $\ell(s) = k_p/(Ls)$. Then, the closed-loop transfer function, that is, $\ell(s)/(1 + \ell(s))$, becomes

$$\frac{I_d(s)}{I_{dref}(s)} = G_i(s) = \frac{1}{\tau_i s + 1}, \qquad k_p = L/\tau_i, \quad k_i = (R + r_{on})/\tau_i.$$

τ_i should be made small for a fast current-control response but adequately large such that $1/\tau_i$, that is, the bandwidth of the closed-loop control system, is considerably smaller, for example, 10 times, than the switching frequency of the VSC (expressed in rad/s).Depending on the requirements of a specific application and the converter switching frequency, τ_i is typically selected in the range of 0.5–5 ms.

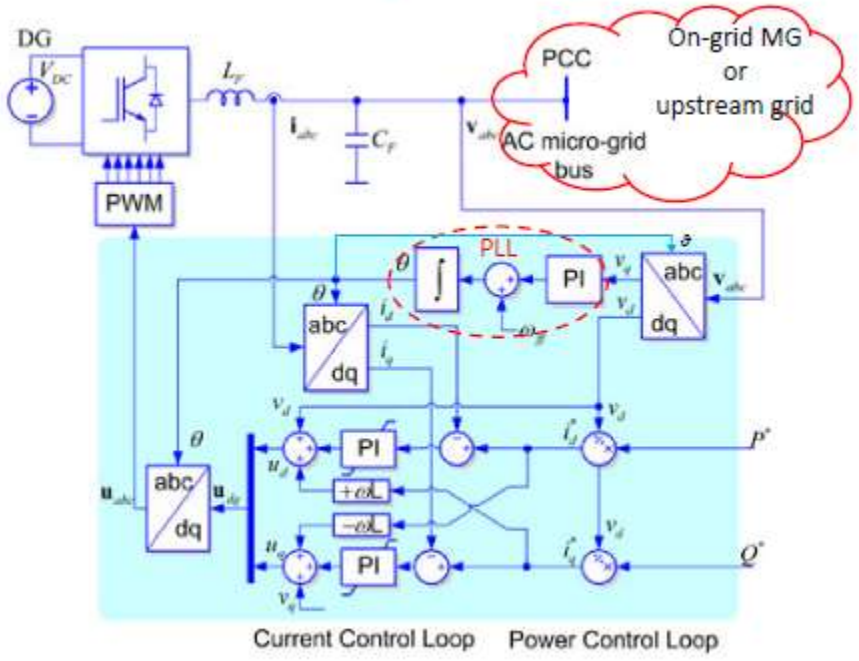

Consider the real-/reactive-power controller of Figure 8.3 with parameters $L = 100\ \mu H$, $R = 0.75\ m\Omega$, $r_{on} = 0.88\ m\Omega$, $V_d = 1.0\ V$, $V_{DC} = 1250\ V$, and $f_s = 3420$ Hz. The AC system frequency and line-to-line rms voltage are $\omega_0 = 377$ rad/s and 480 V (i.e., $V_{sd} = 391\ V$), respectively. The transfer function of the feed-forward filter is $G_{ff}(s) = 1/(8 \times 10^{-6}s + 1)$. The PLL

$$H(s) = \frac{685.42\left(s^2 + 568{,}516\right)\left(s^2 + 166s + 6889\right)}{s\left(s^2 + 1508s + 568{,}516\right)\left(s^2 + 964s + 232{,}324\right)}$$

Assuming a closed-loop time constant of $\tau_i = 2.0$ ms

$$k_d(s) = k_q(s) = \frac{0.05s + 0.815}{s} \quad [\Omega].$$

At t=0.15s, the gating pulses are unblocked and the controllers are activated, while Psref=Qsref≡0. At t=0.20s, Psref is subjected to a step change from 0 to 2.5 MW. At t=0.30s, Psref is subjected to another step change from 2.5 to −2.5MW. At t=0.35s, Qsref is subjected to a step change from 0 to 1.0 MVAr.

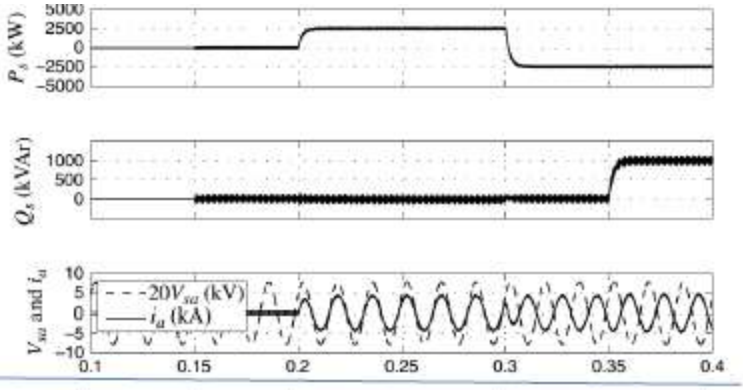

Figure confirms that id and iq are well decoupled; it is observed that iq remains regulated at zero while id is changing from zero to 4.26kA. Ripples on the waveforms of id and iq are due to the pulse-width modulation (PWM) switching side-band harmonics of VSC AC-side currents, which are modulated by 60 Hz via the abc- to dq-frame transformation.

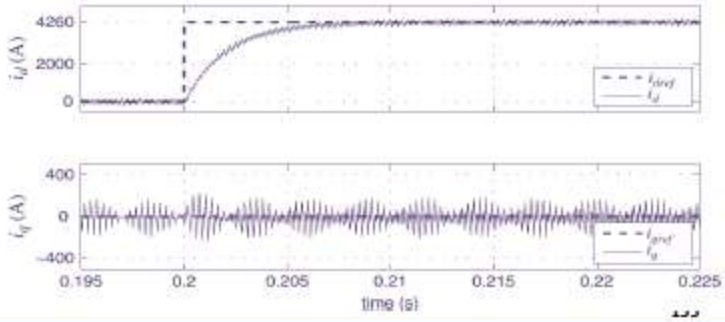

The synchronization system *slowly varies the phase angle and frequency* of the island's voltage to resynchronize with the grid voltage. All the grid-feeding power converters connected to such microgrid would be subjected to the reconnection frequency and phase angle transients, so that this maneuver has to be made in a stable and secure way.

The *phase-locked loop (PLL)* technology has extensively been used to synchronize grid-connected power converters with the grid voltage.

The grid-forming power converters can be represented as an ideal ac voltage source with a low-output impedance, setting the voltage amplitude E∗ and frequency ω∗ of the local grid by using a proper control loop.

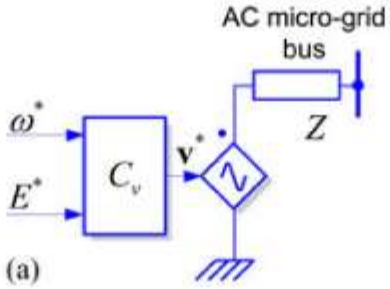

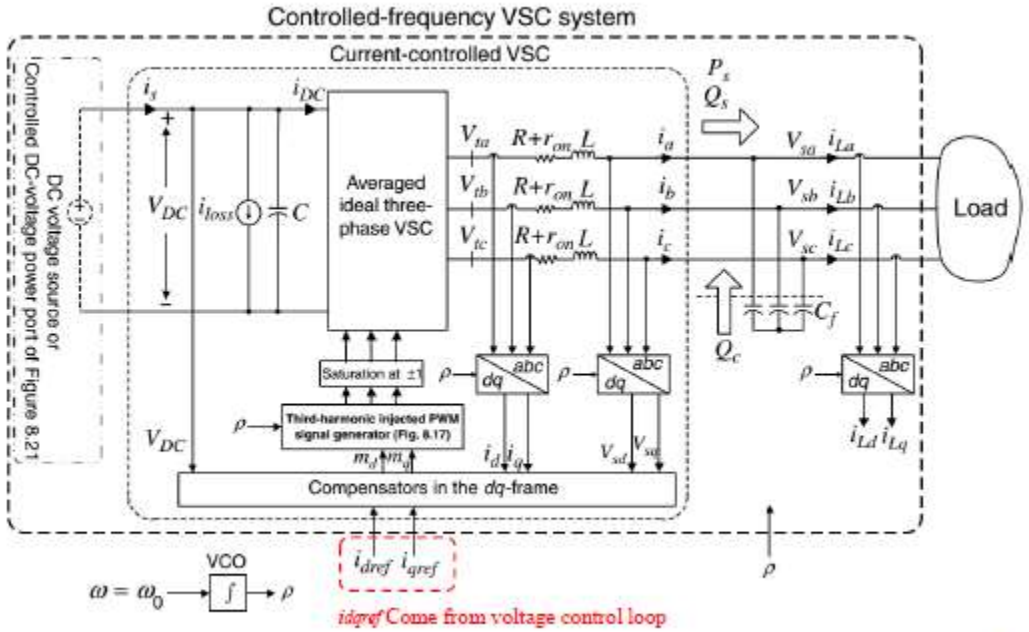

each phase of the VSC AC-side terminals is interfaced with a three-phase load via an interface RLC filter. Thus, the control objective is to regulate the amplitude and frequency of the load voltage, V_{sabc}, in the presence of disturbances in the load current, i_{Labc}. The RLC filter is composed of a series RL branch and a shunt capacitor, C_f.

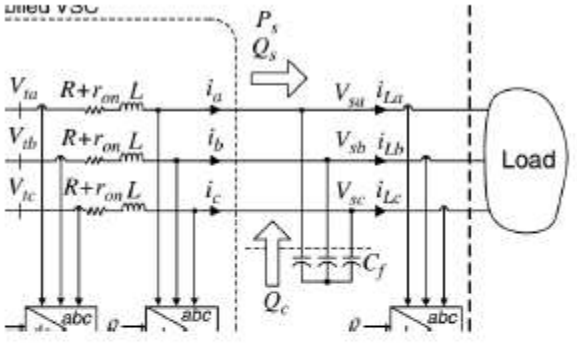

Cf: if load dynamic is known and the controller is designed regard with load dynamic then Cf is not required. But, if controller design must be implemented regardless load configuration and dynamic, Cf is required to ensure that the RL branch is terminated to a node with some degree of voltage support. Cf provides a low-impedance path for switching current harmonics generated by the VSC and thus prevents them from penetrating into the load. Without Cf , harmonic distortion of load voltage, Vsabc, will significantly depend on load impedance at the switching frequency and its harmonics.

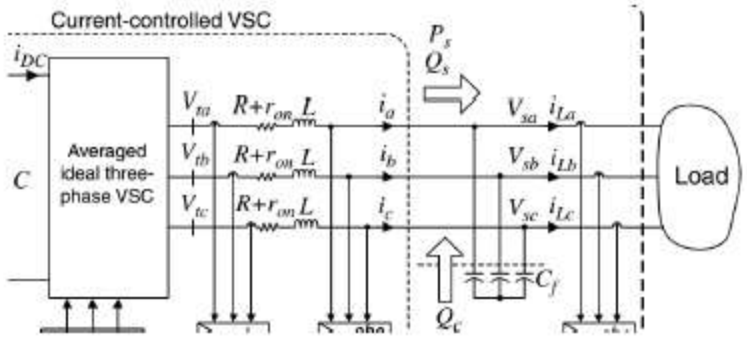

The current-controlled VSC and the filter capacitor deliver the real and reactive power (Ps, Qs) and (0, Qc), respectively. Therefore, the effective power output of the controlled-frequency VSC system of above figure, delivered to the load, is (Ps, Qs + Qc).

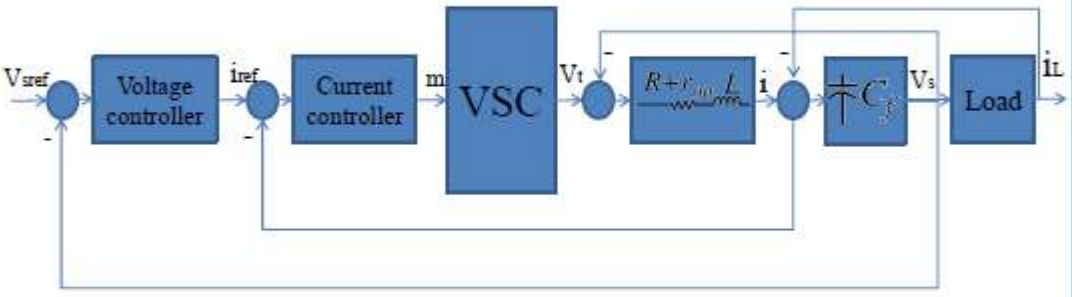

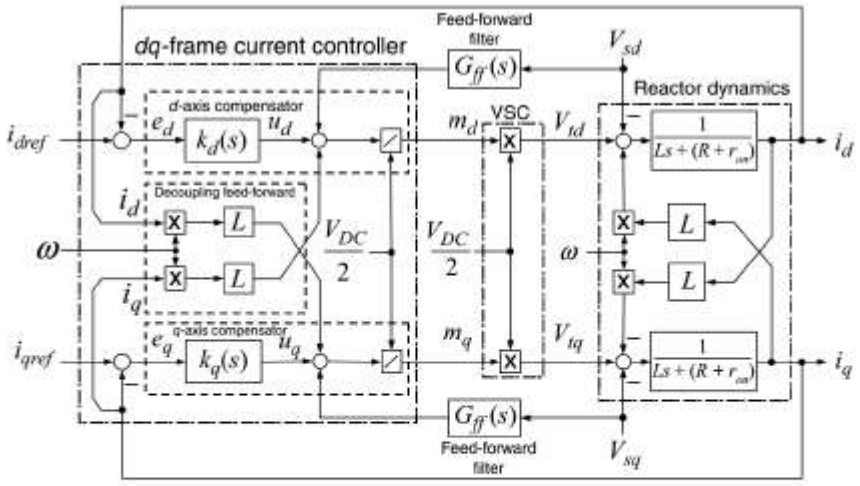

$$k_d(s) = k_q(s) = \frac{k_p s + k_i}{s}.$$

$$k_p = L/\tau_i,$$

$$k_i = (R + r_{on})/\tau_i.$$

Closed loop

$$I_d(s) = G_i(s) I_{dref}(s) = \frac{1}{\tau_i s + 1} I_{dref}(s),$$

$$I_q(s) = G_i(s) I_{qref}(s) = \frac{1}{\tau_i s + 1} I_{qref}(s).$$

140

dynamics of the load voltage are described by state-space equations:

$$C_f \frac{dV_{sa}}{dt} = i_a - i_{La},$$

$$C_f \frac{dV_{sb}}{dt} = i_b - i_{Lb},$$

$$C_f \frac{dV_{sc}}{dt} = i_c - i_{Lc}.$$

$$\longrightarrow \quad C_f \frac{d\vec{V}_s}{dt} = \vec{i} - \vec{i}_L.$$

$$\vec{f} = (f_d + j f_q) e^{j\rho(t)}$$

$$C_f \frac{d}{dt}\left[\left(V_{sd} + jV_{sq}\right) e^{j\rho}\right] = \left(i_d + j i_q\right) e^{j\rho} - \left(i_{Ld} + j i_{Lq}\right) e^{j\rho}.$$

$$\frac{d\rho}{dt} = \omega(t). \longrightarrow \begin{cases} C_f \dfrac{dV_{sd}}{dt} = C_f(\omega V_{sq}) + i_d - i_{Ld} \\ C_f \dfrac{dV_{sq}}{dt} = -C_f(\omega V_{sd}) + i_q - i_{Lq} \end{cases}$$

If the load is an ideal, independent, current-sourced load for which i_{Ld} and i_{Lq} are independent of V_{sd}, V_{sq}, and ω and can be assumed as disturbances or inputs.

141

Generally, the load current components, that is, iLd and iLq, can be regarded as outputs of a dynamic system whose inputs are Vsd and Vsq. Thus,

$$\begin{bmatrix} i_{Ld} \\ i_{Lq} \end{bmatrix} = \begin{bmatrix} g_1(x_1, x_2, \ldots, x_n, V_{sd}, V_{sq}, \omega, t) \\ g_2(x_1, x_2, \ldots, x_n, V_{sd}, V_{sq}, \omega, t) \end{bmatrix},$$

where x1(t), . . . , xn(t) are the state variables, and g1(·) and g2(·) are nonlinear functions of their arguments. Dynamics of the state variables are governed by the equation

$$\frac{d}{dt}\begin{bmatrix} x_1 \\ x_2 \\ \cdot \\ \cdot \\ \cdot \\ x_n \end{bmatrix} = \begin{bmatrix} f_1(x_1, x_2, \ldots, x_n, V_{sd}, V_{sq}, \omega, t) \\ f_2(x_1, x_2, \ldots, x_n, V_{sd}, V_{sq}, \omega, t) \\ \cdot \\ \cdot \\ \cdot \\ f_n(x_1, x_2, \ldots, x_n, V_{sd}, V_{sq}, \omega, t) \end{bmatrix},$$

where f1(·), . . . , fn(·) are nonlinear functions of their arguments.

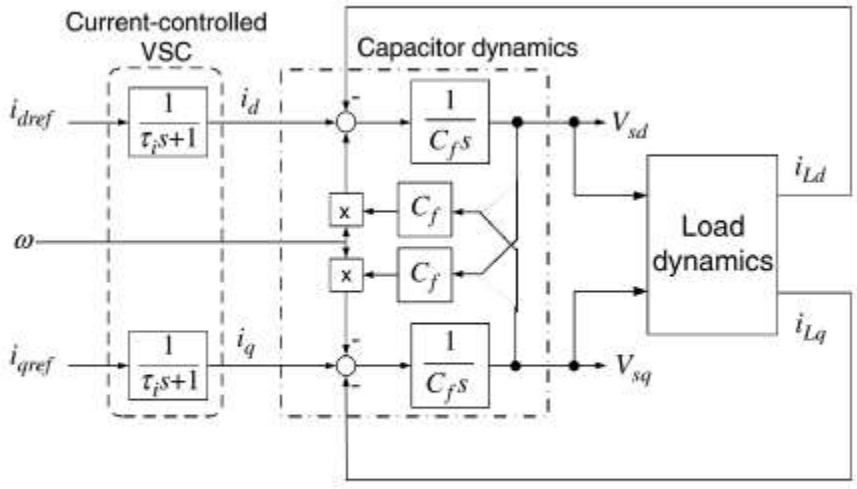

$$L_1\frac{di_{1a}}{dt} = -R_1 i_{1a} + V_{sa} - V_{n1},$$
$$L_1\frac{di_{1b}}{dt} = -R_1 i_{1b} + V_{sb} - V_{n1},$$
$$L_1\frac{di_{1c}}{dt} = -R_1 i_{1c} + V_{sc} - V_{n1},$$
$$\rightarrow L_1\frac{d\vec{i}_1}{dt} = -R_1\vec{i}_1 + \vec{V}_s.$$

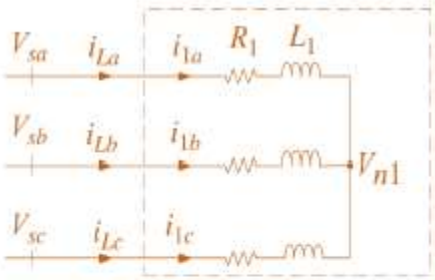

$$L_1\frac{d\vec{i}_1}{dt} = -R_1\vec{i}_1 + \vec{V}_s.$$

State space equation

$$\frac{di_{1d}}{dt} = -\frac{R_1}{L_1}i_{1d} + \omega i_{1q} + \frac{1}{L_1}V_{sd} = f_1(i_{1d}, i_{1q}, V_{sd}, V_{sq}),$$
$$\frac{di_{1q}}{dt} = -\omega i_{1d} - \frac{R_1}{L_1}i_{1q} + \frac{1}{L_1}V_{sq} = f_2(i_{1d}, i_{1q}, V_{sd}, V_{sq}).$$

Output equation

$$i_{Ld} = i_{1d} = g_1(i_{1d}, i_{1q}, V_{sd}, V_{sq}),$$
$$i_{Lq} = i_{1q} = g_2(i_{1d}, i_{1q}, V_{sd}, V_{sq}).$$

in general, the dynamic system representing this load has two state variables, three inputs, and two outputs. It is interesting to note that even if ω(t) is a variable, system has nonlinear.

The control objective for the controlled-frequency VSC system is to regulate the amplitude and the frequency of the load voltage, Vsabc.

Vsref

$$V_{sa}(t) = \widehat{V}_s\cos(\omega_0 t + \theta_0),$$
$$V_{sb}(t) = \widehat{V}_s\cos\left(\omega_0 t + \theta_0 - \frac{2\pi}{3}\right),$$
$$V_{sc}(t) = \widehat{V}_s\cos\left(\omega_0 t + \theta_0 - \frac{4\pi}{3}\right),$$

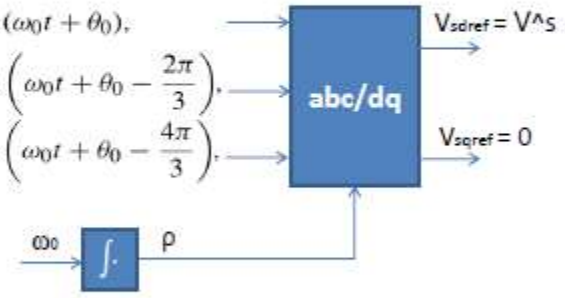

The block diagram suggests that V_{sd} and V_{sq} can be controlled by i_{dref} and i_{qref} .

the system includes the impacts of iLd and iLq. As shown before, even for simple linear configurations, the load dynamic model is typically of a high order, strongly intercoupled, time varying, and even nonlinear. Consequently, the design of a control scheme for this system that guarantees the closed-loop stability or fulfills a prespecified dynamic performance is not a straightforward task.

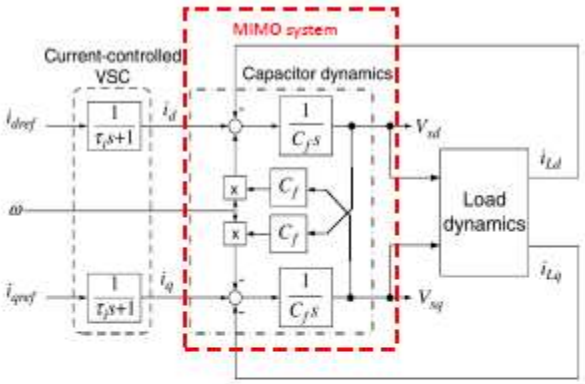

$$C_f \frac{dV_{sd}}{dt} = C_f(\omega V_{sq}) + i_d - i_{Ld}$$

$$C_f \frac{dV_{sq}}{dt} = -C_f(\omega V_{sd}) + i_q - i_{Lq}$$

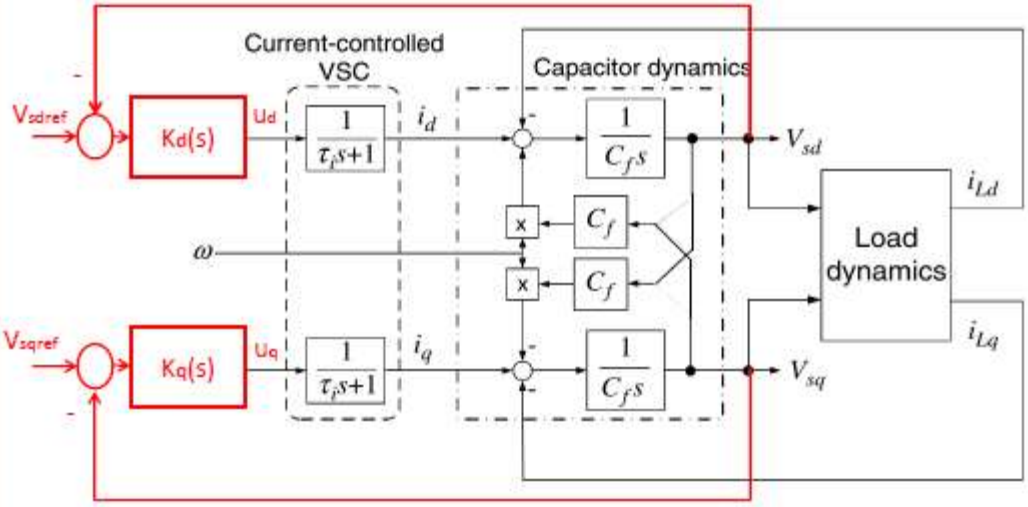

the coupling between V_{sd} and V_{sq} is eliminated by a decoupling feed-forward compensation . The feed-forward compensation is similar to the one utilized to decouple *id* and *iq* in a current-controlled VSC and makes it possible to control V_{sd} by i_{dref} and V_{sq} by i_{qref}.

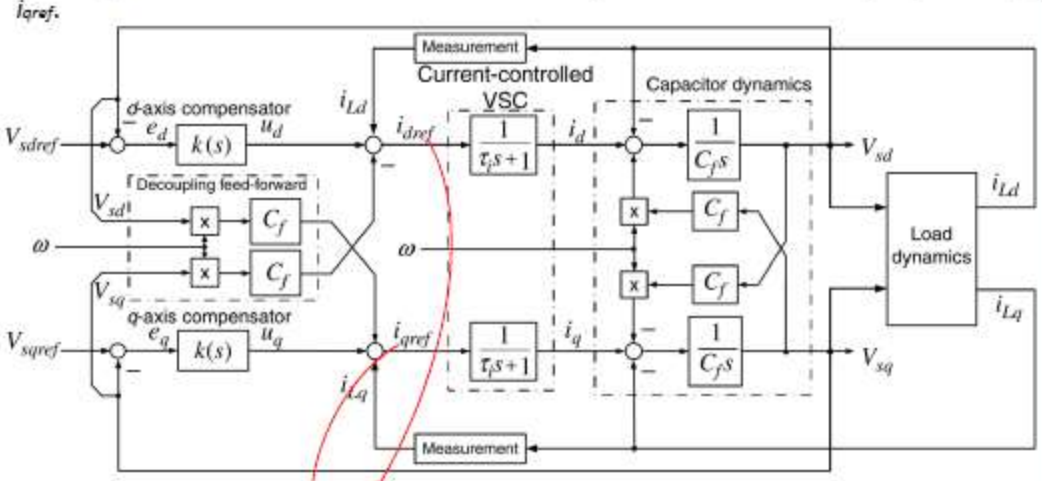

$$i_{dref} = u_d - C_f(\omega V_{sq}) + i_{Ld},$$

$$i_{qref} = u_q + C_f(\omega V_{sd}) + i_{Lq}.$$

Transfer function $\frac{V_{sd}(s)}{U_d(s)}$ and $\frac{V_{sq}(s)}{U_q(s)}$:

$$I_d(s) = G_i(s)U_d(s) - C_f G_i(s) \pounds \{\omega V_{sq}\} + G_i(s)I_{Ld}(s),$$

$$I_q(s) = G_i(s)U_q(s) + C_f G_i(s) \pounds \{\omega V_{sd}\} + G_i(s)I_{Lq}(s),$$

$$C_f \frac{dV_{sd}}{dt} = C_f(\omega V_{sq}) + i_d - i_{Ld} \xrightarrow{\text{Laplacian}} C_f s V_{sd} = C_f \mathcal{L}\{\omega V_{sq}\} + I_d(s) - I_{Ld}(s)$$

$$C_f \frac{dV_{sq}}{dt} = -C_f(\omega V_{sd}) + i_q - i_{Lq}, \qquad C_f s V_{sq} = -C_f \mathcal{L}\{\omega V_{sd}\} + I_q(s) - I_{Lq}(s)$$

$$C_f s V_{sd}(s) = G_i(s)U_d(s) + C_f[1 - G_i(s)] \pounds \{\omega V_{sq}\} - [1 - G_i(s)]I_{Ld}(s),$$

$$C_f s V_{sq}(s) = G_i(s)U_q(s) - C_f[1 - G_i(s)] \pounds \{\omega V_{sd}\} - [1 - G_i(s)]I_{Lq}(s).$$

$G_i(s) = 1/(\tau_i s + 1)$ — has a unity DC gain

$[1 - G_i(s)] = \tau_i s/(\tau_i s + 1)$ — has a zero DC gain

If τ_i is small, $[1 - G_i(s)]$ is insignificant over a relatively wide range of frequencies and can be approximated by zero.

$$C_f s V_{sd}(s) = G_i(s)U_d(s) + C_f[1 - G_i(s)] \pounds \{\omega V_{sq}\} - [1 - G_i(s)]I_{Ld}(s), \qquad \frac{V_{sd}(s)}{U_d(s)} \approx G_i(s)\frac{1}{C_f s},$$

$$C_f s V_{sq}(s) = G_i(s)U_q(s) - C_f[1 - G_i(s)] \pounds \{\omega V_{sd}\} - [1 - G_i(s)]I_{Lq}(s). \qquad \frac{V_{sq}(s)}{U_q(s)} \approx G_i(s)\frac{1}{C_f s},$$

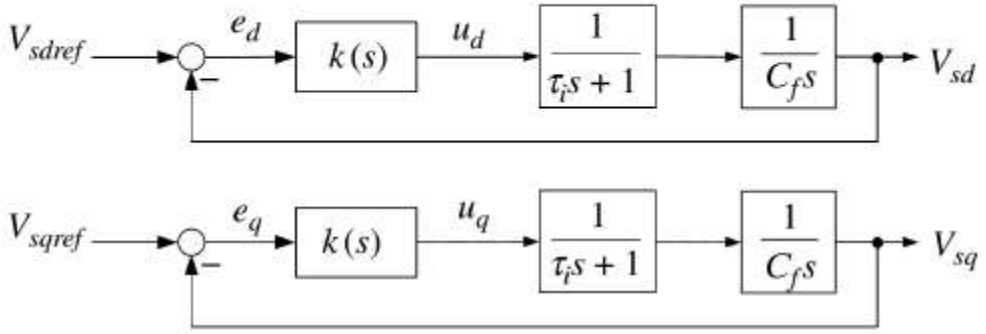

Figures represent two, linear, decoupled systems (two SISO system). The first compensator processes $e_d = V_{sdref} - V_{sd}$ and generates u_d. The other compensator processes $e_q = V_{sqref} - V_{sq}$ and generates u_q. Then, i_{dref} and i_{qref} are constructed from u_d and u_q and delivered to the corresponding d- and q-axis current-control loops.

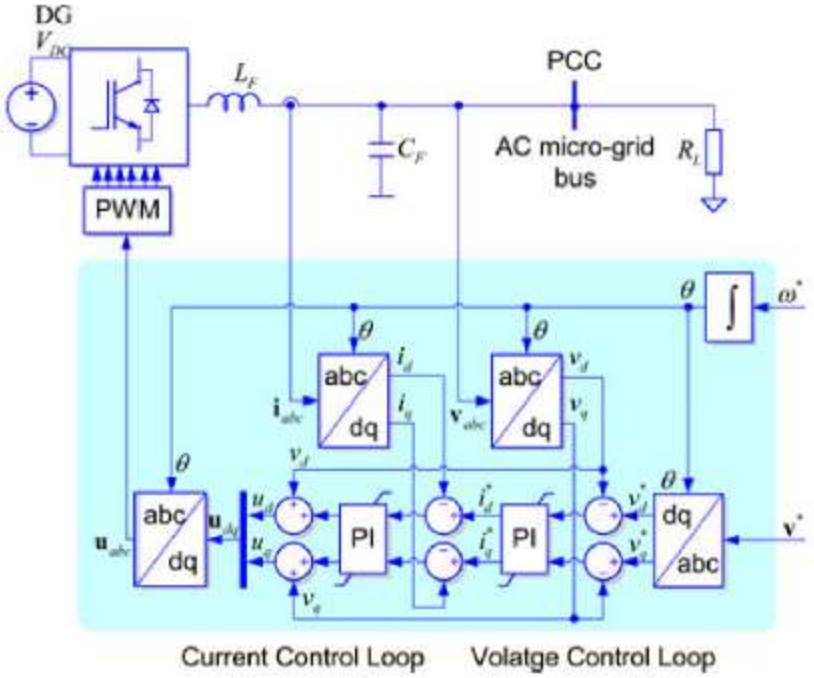

Each of the d- and q-axis control loops shown in Figure includes one integral term, that is, one pole at s = 0, in addition to the real pole at s = −1/τi. For a system of this type, the simplest compensator to fulfill fast regulation and zero steady-state error is a PI compensator. Let the PI compensator be

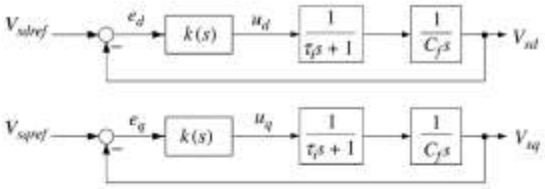

$$k(s) = k\frac{s+z}{s}. \xrightarrow{\text{Loop gain}} \ell(s) = \frac{k}{\tau_i C_f}\left(\frac{s+z}{s+\tau_i^{-1}}\right)\frac{1}{s^2}.$$

At low frequencies, ∠l(jω) ≈ −180◦ due to the double pole at s = 0. If z < τi^−1, ∠l(jω) first increases until it reaches a maximum, δm, at a certain frequency, ωm. Then, for ω > ωm, ∠l(jω) drops and asymptotically approaches −180◦. δm and ωm are given by

$$\delta_m = \sin^{-1}\left(\frac{1-\tau_i z}{1+\tau_i z}\right) \qquad \omega_m = \sqrt{z\tau_i^{-1}}.$$

If the gain crossover frequency ωc is chosen as ωm, then δm becomes the phase margin. In order for this to hold, the compensator proportional gain, k, must satisfy the condition |l(jωc)| = |l(jωm)| = 1. This yields $k = C_f\omega_c$.

$$\left.\begin{aligned}\ell(s) &= \frac{k}{\tau_i C_f}\left(\frac{s+z}{s+\tau_i^{-1}}\right)\frac{1}{s^2}\\ G_{cl}(s) &= \frac{\ell(s)}{1+\ell(s)}\end{aligned}\right\} \xrightarrow{\tau_i^{-1}=p} G_{cl}(s) = \frac{k(s+z)}{\frac{C_f}{p}(s+p)s^2 + k(s+z)}$$

$$\frac{C_f}{p}(s+p)s^2 + k(s+z) = 0 \quad \rightarrow \quad s^3 + ps^2 + \frac{kp}{C_f}(s+z) = 0$$

$$\xrightarrow{\frac{k}{C_f}=\omega_c \;,\, pz=\omega_c^2} s^3 + ps^2 + \frac{kp}{C_f}(s+z) = (s+\omega_c)(s^2 + \underbrace{(p-\omega_c)}_{2\xi\omega_n}s + \underbrace{\omega_c^2}_{\omega_n^2}) = 0$$

Based on this method, the resultant closed-loop system is of the third order. It was shown that the closed-loop system always has one real pole at s = −ωc in addition to two other (complex-conjugate) poles that are located on a circle with a radius of ωc.

$p-\omega_c = 2\omega_c \rightarrow (s^2 + (p-\omega_c)s + \omega_c^2) = (s+\omega_c)^2 \rightarrow s_{2,3} = -\omega_c$

$p-\omega_c = 2\frac{\sqrt{2}}{2}\omega_c \rightarrow (s^2 + (p-\omega_c)s + \omega_c^2) = (s^2 + \sqrt{2}\omega_c s + \omega_c^2) = 0 \rightarrow s_{2,3} = -\frac{\sqrt{2}}{2}\omega_c \pm j\frac{\sqrt{2}}{2}\omega_c$

$p - \omega_c = 2\omega_c \rightarrow p = 3\omega_c \rightarrow p = 3\sqrt{pz} \rightarrow p = 9z \rightarrow \delta_m = 53^\circ @\omega_c$ δ_m=phase margin

$p - \omega_c = 2\frac{\sqrt{2}}{2}\omega_c \rightarrow p = (1+\sqrt{2})\omega_c \rightarrow p = (1+\sqrt{2})\sqrt{pz} \rightarrow p = 5.8z \rightarrow \delta_m = 45^\circ @\omega_c$

The exact locations of the two poles on the circle depend on the selected phase margin that, typically, is selected between 30◦ and 75◦. Two particular choices of interest are :

1) a phase margin of $\delta_m = 45^\circ$, and
2) a phase margin of $\delta_m = 53^\circ$, which makes the two poles coincide with $s = -\omega_c$. With tis choice, the closed-loop system will have a triple pole at $s = -\omega_c$.

the grid-supporting converters can be represented either as an ideal ac-controlled current source in parallel with a shunt impedance, or as an ideal ac voltage source in series with a link impedance. These converters regulate their output current/voltage to keep the value of the grid frequency and voltage amplitude close to their rated values. In any case, its main objective is to participate in the regulation of the ac grid voltage amplitude $\underline{E}$ and frequency $\underline{\omega}$ by controlling the active and reactive power delivered to the grid.

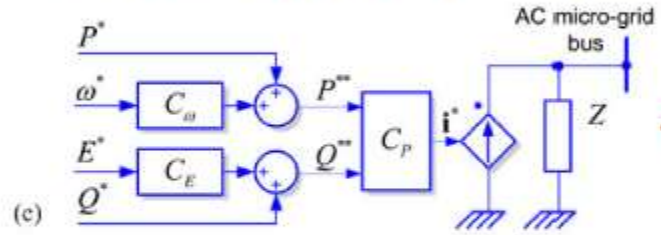

(c)

→ This scheme must be used in grid-connected mode with a grid-forming converter/SG in the MG.

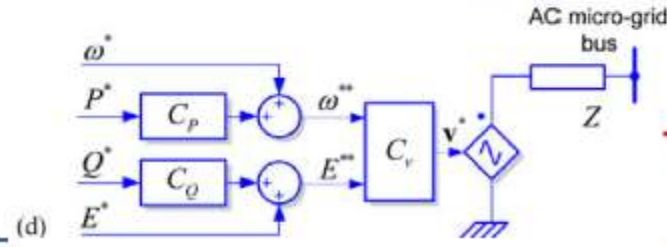

(d)

→ This scheme can be used in grid-connected and islanded mode same as SG.

Problem: Different current sharing strategies have been proposed for small rated paralleled inverters.

Method: such as centralized controllers, master–slave, average-load sharing, or circular-chain controls.

Difficulty: However, these solutions are conceived for paralleling systems which are close to each other and interconnected through high-bandwidth communication channels used for control purposes. These communication-based solutions are not the most suitable choice for controlling microgrids, since distributed generators and loads in microgrids may be separated several kilometers.

Solution: To overcome this problem, **droop control** algorithms are used to control the power sharing in microgrids without using communication channels, thereby eliminating the limits imposed by the physical location and improving the microgrid performance. The droop regulation techniques are implemented in grid-supporting power converters to regulate the exchange of active and reactive powers with the grid, in order to keep the grid voltage frequency and amplitude under control.

Main idea: The main idea to support the droop control comes from mimic the self-regulation capability of the synchronous generator in grid-connection mode, decreasing the delivered active power when the grid frequency increases and decreasing the injected reactive power when the grid voltage amplitude increases.

Considering the power converter as an ideal controllable voltage source that is connected to the mains through a given line impedance, as shown in Figure, the active and reactive powers that it will deliver to the grid can be written as:

$$S_A = \hat{V}_A \hat{I}^* = \hat{V}_A \left(\frac{\hat{V}_A - \hat{V}_B}{R + jX} \right)^* = P_A + jQ_A$$

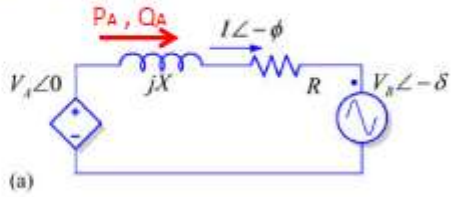

$$P_A = \frac{V_A}{R^2 + X^2} \left[R \left(V_A - V_B \cos\delta \right) + X V_B \sin\delta \right]$$

$$Q_A = \frac{V_A}{R^2 + X^2} \left[-R V_B \sin\delta + X \left(V_A - V_B \cos\delta \right) \right].$$

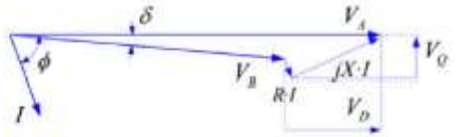

Grid Impedance Influence on Droop Control: Inductive grid

The inductive component of the line impedances in HV and MV networks is typically much higher than the resistive one, as shown in Table.

TYPICAL LINE IMPEDANCES VALUES

Type of Line	R (Ω/km)	X (Ω/km)	R/X (p.u.)
Low Voltage Line	0.642	0.083	7.7
Medium Voltage Line	0.161	0.190	0.85
High Voltage Line	0.06	0.191	0.31

Therefore, the resistive part can be neglected without making any significant error. In addition, the power angle δ in such lines is small, so it can be assumed that sin(δ) ≈ δ and cos(δ) ≈ 1 . Therefore:

$$P_A = \frac{V_A}{R^2 + X^2} \left[R \left(V_A - V_B \cos\delta \right) + X V_B \sin\delta \right] \longrightarrow P_A \approx \frac{V_A}{X} \left(V_B \sin\delta \right) \Rightarrow \delta \approx \frac{X P_A}{V_A V_B}$$

$$Q_A = \frac{V_A}{R^2 + X^2} \left[-R V_B \sin\delta + X \left(V_A - V_B \cos\delta \right) \right]. \qquad Q_A \approx \frac{V_A}{X} \left(V_A - V_B \cos\delta \right) \Rightarrow V_A - V_B \approx \frac{X Q_A}{V_A}.$$

Expressions show a direct relationship between the power angle δ and the active power P, as well as between the voltage difference VA – VB and the reactive power Q.

$$P_A \approx \frac{V_A}{X}(V_B \sin\delta) \Rightarrow \delta \approx \frac{XP_A}{V_A V_B}$$

$$Q_A \approx \frac{V_A}{X}(V_A - V_B \cos\delta) \Rightarrow V_A - V_B \approx \frac{XQ_A}{V_A}.$$

These relationships permit two regulating problem:

1) regulating the grid frequency and voltage at the point of connection of the power converter, by controlling the value of the active and reactive powers delivered to the grid.

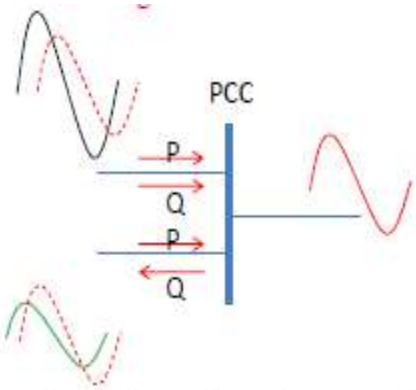

2) regulating the active and reactive powers delivered to the grid at the point of connection of the power converter, by controlling the value of the grid frequency and voltage.

Therefore, the following droop control expressions can be written for inductive lines:

$$f - f_O = -k_p (P - P_O)$$

$$V - V_O = -k_q (Q - Q_O)$$

fo , Vo , Po , Qo are rated values.

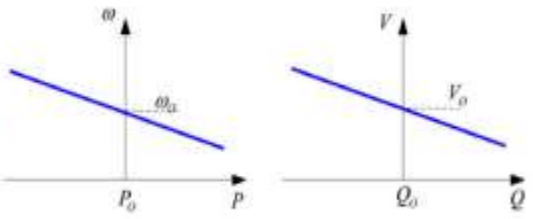

1) regulating the grid frequency and voltage at the point of connection of the power converter, by controlling the value of the active and reactive powers delivered to the grid.

$$f^* - f_O = -k_p\,(P^* - P_O)$$
$$V - V_O = -k_q\,(Q^* - Q_O)$$

2) regulating the active and reactive powers delivered to the grid at the point of connection of the power converter, by controlling the value of the grid frequency and voltage.

$$f^* - f_O = -k_p\,(P - P_O)$$
$$V^* - V_O = -k_q\,(Q - Q_O)$$

1) regulating the grid frequency and voltage at the point of connection of the power converter, by controlling the value of the active and reactive powers delivered to the grid.

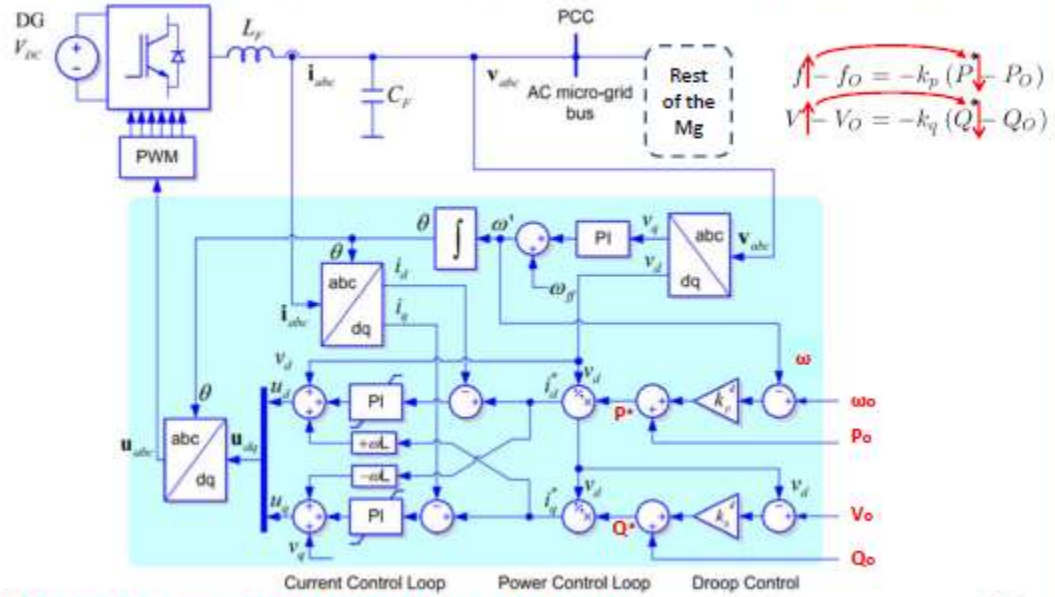

Grid-supporting power converter operating as a current source.

2) regulating the active and reactive powers delivered to the grid at the point of connection of the power converter, by controlling the value of the grid frequency and voltage.

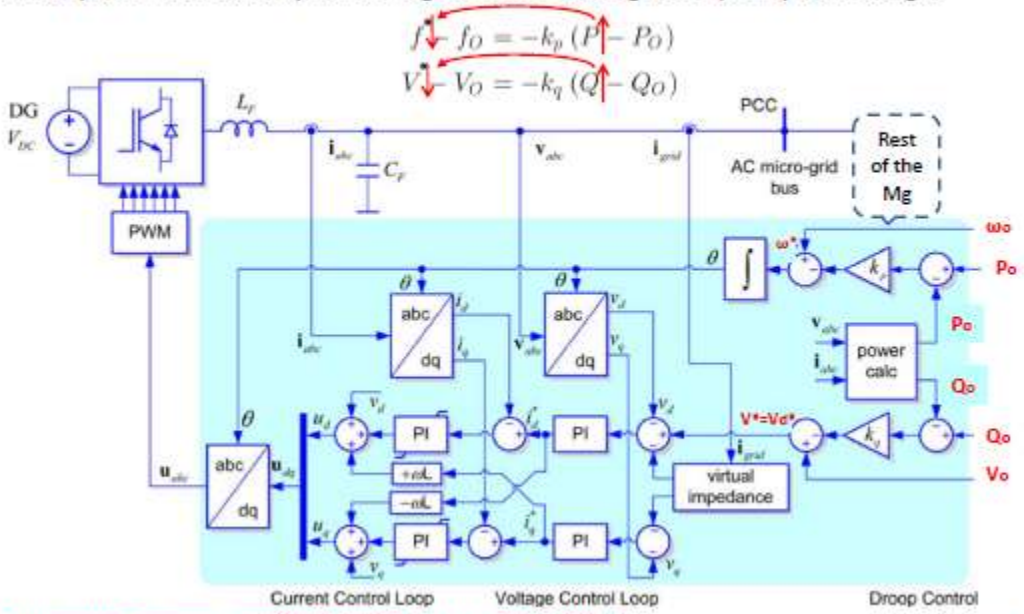

Gridsupporting power converter operating as a voltage source.

On the contrary to the case of HV networks, the grid impedance in LV networks is mainly resistive, and thus, the inductive part can be neglected. As a consequence, and maintaining the assumption that the power angle δ has a small value:

$$P_A = \frac{V_A}{R^2 + X^2}\left[R\left(V_A - V_B\cos\delta\right) + XV_B\sin\delta\right]$$
$$Q_A = \frac{V_A}{R^2 + X^2}\left[-RV_B\sin\delta + X\left(V_A - V_B\cos\delta\right)\right].$$

$$\longrightarrow$$

$$P_A \approx \frac{V_A}{R}\left(V_A - V_B\cos\delta\right) \Rightarrow V_A - V_B \approx \frac{RP_A}{V_A}$$
$$Q_A = -\frac{V_A \cdot V_B}{R}\sin\delta \Rightarrow \delta \approx -\frac{RQ_A}{V_A V_B}.$$

Expressions show a direct relationship between the power angle δ and the reactive power Q, as well as between the voltage difference $V_A - V_B$ and the active power P.

$$P_A \approx \frac{V_A}{R}\left(V_A - V_B \cos\delta\right) \Rightarrow V_A - V_B \approx \frac{RP_A}{V_A}$$

$$Q_A = -\frac{V_A \cdot V_B}{R}\sin\delta \Rightarrow \delta \approx -\frac{RQ_A}{V_A V_B}.$$

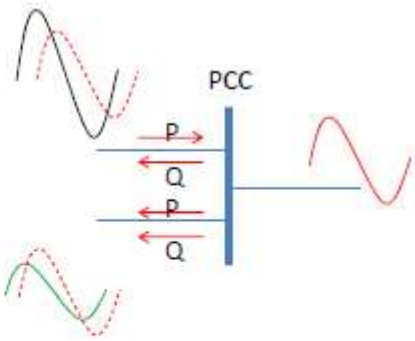

The following droop control expressions can be written for resistive lines:

$$V - V_O = -k_p\left(P - P_O\right)$$

$$f - f_O = k_q\left(Q - Q_O\right)$$

fo , Vo , Po , Qo are rated values.

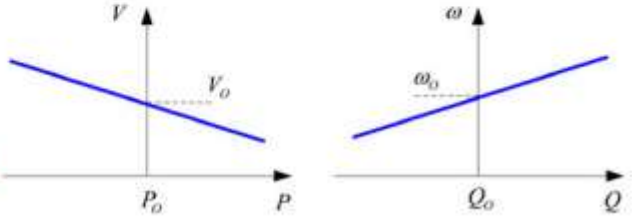

In the general case, the combined effect of the resistive and inductive line impedance components should be taken into account in the droop control equations.

$Z=|Z|\angle\Theta=|Z|\cos\Theta+j|Z|\sin\Theta=R+jX$

$$P_A = \frac{V_A}{R^2+X^2}\left[R\left(V_A - V_B\cos\delta\right) + XV_B\sin\delta\right]$$

$$Q_A = \frac{V_A}{R^2+X^2}\left[-RV_B\sin\delta + X\left(V_A - V_B\cos\delta\right)\right].$$

$\Theta=\pi/2 \rightarrow Z=X$

$$P_A \approx \frac{V_A}{X}\left(V_B\sin\delta\right)$$

$$Q_A \approx \frac{V_A}{X}\left(V_A - V_B\cos\delta\right)$$

$\Theta=0 \rightarrow Z=R$

$$P_A \approx \frac{V_A}{R}\left(V_A - V_B\cos\delta\right)$$

$$Q_A = -\frac{V_A \cdot V_B}{R}\sin\delta$$

To do that, a rotation matrix **T** is used to transform the active and reactive powers, P and Q, into the rotational power components, P' and Q', as detailed in the following:

$$\frac{X}{Z}P_A - \frac{R}{Z}Q_A = \frac{V_A V_B}{Z}sin\delta = P'_A \qquad \frac{R}{Z}P_A + \frac{X}{Z}Q_A = \frac{V_A - V_B\,cos\delta}{Z} = Q'_A$$

$$\begin{bmatrix} P' \\ Q' \end{bmatrix} = \begin{bmatrix} X/Z & -R/Z \\ R/Z & X/Z \end{bmatrix} \cdot \begin{bmatrix} P \\ Q \end{bmatrix} \begin{cases} \frac{X}{Z} = sin\theta = \cos\left(\frac{\pi}{2} - \theta\right) = cos\varphi \\ \frac{R}{Z} = cos\theta = sin\left(\frac{\pi}{2} - \theta\right) = sin\varphi \end{cases}$$

$$\begin{bmatrix} P' \\ Q' \end{bmatrix} = \begin{bmatrix} \cos\phi & -\sin\phi \\ \sin\phi & \cos\phi \end{bmatrix} \cdot \begin{bmatrix} P \\ Q \end{bmatrix} = [\mathbf{T}] \cdot \begin{bmatrix} P \\ Q \end{bmatrix}$$

δ takes a small value, thus:

$$P'_A \approx \frac{V_A}{Z}\left(V_B \sin\delta\right) \Rightarrow \delta \approx \frac{ZP'_A}{V_A V_B}$$

$$Q'_A \approx \frac{V_A}{Z}\left(V_A - V_B \cos\delta\right) \Rightarrow V_A - V_B \approx \frac{ZQ'_A}{V_A}$$

where P'_A and Q'_A are the rotated components of P_A and Q_A. it can be concluded that the power angle δ can be controlled by regulating the rotating active power P'_A, while the voltage difference $V_A - V_B$ can be changed by regulating the rotating reactive power Q'_A. Therefore, in a general case, the droop control equations can be written as:

$$f - f_0 = -k_p\left(P' - P'_0\right) = -k_p\frac{X}{Z}\left(P - P_0\right) + k_q\frac{R}{Z}\left(Q - Q_0\right)$$

$$V - V_0 = -k_q\left(Q' - Q'_0\right) = -k_p\frac{R}{Z}\left(P - P_0\right) - k_q\frac{X}{Z}\left(Q - Q_0\right).$$

According to above equation, the contribution in the compensation of the frequency and the voltage amplitude variations by each grid-supporting power converter in a microgrid can be adjusted by changing the values kp and kq.

$$f - f_0 = -k_p \left(P' - P'_0\right) = -k_p \frac{X}{Z} \left(P - P_0\right) + k_q \frac{R}{Z} \left(Q - Q_0\right)$$
$$V - V_0 = -k_q \left(Q' - Q'_0\right) = -k_p \frac{R}{Z} \left(P - P_0\right) - k_q \frac{X}{Z} \left(Q - Q_0\right).$$

Problem: Conventional P/f and Q/V droop controls have been proven to be an effective solution for regulating the voltage magnitude and frequency in MV networks, where the lines have a predominant inductive behavior. However, as shown previously, the performance of this kind of controls is highly dependent on the R/X ratio of the line. Due to this feature, this method cannot be directly applied in all kind of networks, unless complicated grid impedance estimation algorithms are implemented in order to calculate the rotated powers indicated above. This issue is even more important when the droop control is applied to LV microgrids. In such a case, a small mismatching in the grid impedance estimation results in an inefficient power sharing among the droop controlled distributed generators.

Solution: As an intuitive solution to solve these drawbacks, resulting from the strong dependence of the conventional droop controller performance on the line impedance value, large inductors could be used to link the power converter to the ac bus and thereby the line impedance would be predominantly inductive. However, this is not an efficient solution since, in addition to the increase in the size and the costs, the dc-bus voltage level should be significantly increased to compensate the high voltage drop across these inductors, thus reducing the overall efficiency. A more effective solution consists on introducing virtually the effect of this link impedance, adapting the control loop of the power converter in order to include its effect.

Note: It is worth to remark that the value of the virtual impedance should be larger than the actual line impedance; otherwise, it will not have a predominant effect in the power flow equations.

The virtual impedance modifies the power converter output voltage reference where the modified voltage reference v_{ref} is obtained by subtracting the virtual voltage drop across the virtual impedance ($Z_v \cdot i_{grid}$) from the reference value originally provided by the droop equations, v_{ref}^* :

$$\boldsymbol{v}_{\mathrm{ref}} = \boldsymbol{v}_{\mathrm{ref}}^{*} - Z_V \cdot \boldsymbol{i}_{\mathrm{grid}} .$$

The value of Z_v sets the dynamic of the controller; hence, it must be considered as a control variable and should be selected according to the nominal power of the converter.

Block diagram of the virtual output impedance loop working with P and Q droop method in the grid power converter.

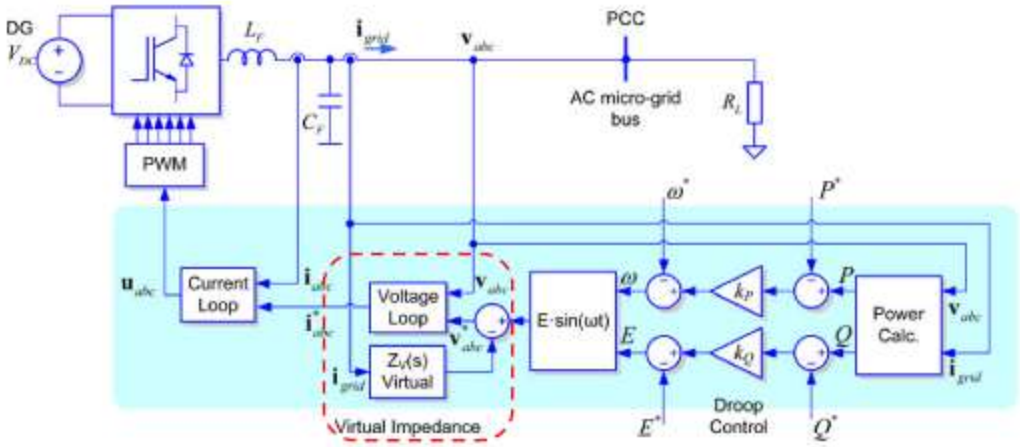

In a microgrid, where different power generation systems based on different technologies and power ratings are interconnected, it is necessary to implement a hierarchical control structure oriented to minimize the operation cost, while maximizing efficiency, reliability, and controllability.
Power ratings, distribution of loads and generation systems, electrical market prices, generation costs, and energy availability from stochastic primary sources are the main issues to be considered when determining the optimum operation point of a microgrid.

Hierarchical control of microgrids can be organized into three main layers:
1) Primary control
2) Secondary control
3) tertiary control

The primary control, the so-called local control, is devoted to control local variables, such as frequency and voltage, as well as current injection. In addition to other low-level controls, these local controllers deal with implementing droop and virtual inductance control techniques in each of the distributed power converters connected to the microgrid.

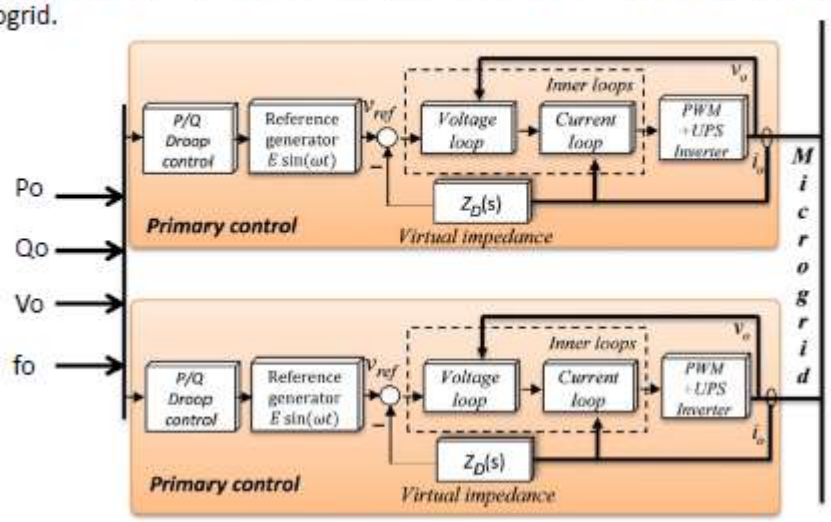

The secondary control ensures that the frequency and voltage deviations are regulated toward zero after every change of load or generation inside the MG. The frequency and amplitude levels in the MG, ω_{MG} and E_{MG}, are sensed and compared with the references ω^*_{MG} and E^*_{MG} ; the errors processed through the compensators ($\delta\omega$ and δE) are sent to all the units to restore the output-voltage frequency and amplitude.

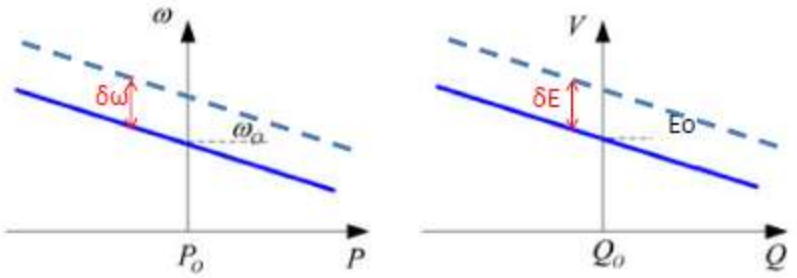

$\omega' = \omega_o + \delta\omega$ $\quad$ $E' = E_o + \delta E$

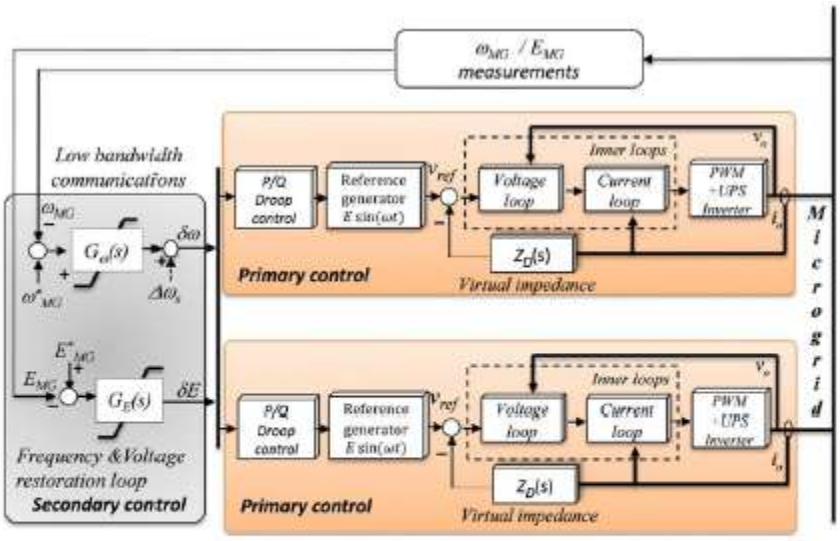

The secondary control makes use of communications and wide-area monitoring (WAM) systems to coordinate the action of all the generation units within a given area, being its time response in the range of minutes, thus having a slow dynamic if compared with the primary control.

In case of an ac MG, the frequency and amplitude restoration controllers G_ω and G_E, shown in Figure, can be obtained similarly as follows :

$$\delta\omega = k_{p\omega}\left(\omega^*_{\mathrm{MG}} - \omega_{\mathrm{MG}}\right) + k_{i\omega}\int\left(\omega^*_{\mathrm{MG}} - \omega_{\mathrm{MG}}\right)dt + \Delta\omega_S$$

$$\delta E = k_{pE}\left(E^*_{\mathrm{MG}} - E_{\mathrm{MG}}\right) + k_{iE}\int\left(E^*_{\mathrm{MG}} - E_{\mathrm{MG}}\right)dt$$

PI controller with time constant

where $k_{p\omega}$, $k_{i\omega}$, k_{pE}, and k_{iE} are the control parameters of the secondary-control compensator. In this case, $\delta\omega$ and δE must be limited in order not to exceed the maximum allowed frequency and amplitude deviations.

$\Delta\omega_s$: is a synchronization term which remains equal to zero when the grid is not present. In order to connect the MG to the grid, we have to measure the frequency and voltage of the grid, and that will be the reference of the secondary control loop. The phase between the grid and the MG will be synchronized by means of the synchronization control loop which can be seen as a conventional PLL. The output signal of the PLL, $\Delta\omega_s$ will be added to the secondary control and will be sent to all the modules to synchronize the MG phase. After several line cycles, the synchronization process will have finished and the MG can be connected to the mains through the static bypass switch. At that moment, the MG does not have any exchange of power with the mains.

When the MG is operating in grid-connected mode, the power flow can be controlled by adjusting the frequency (changing the phase in steady state) and amplitude of the voltage inside the MG

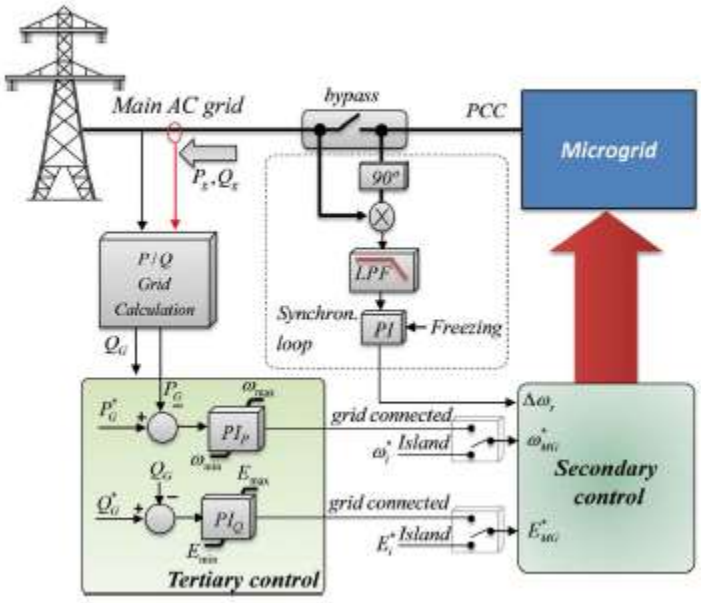

As can be seen in the tertiary control block diagram of Figure, by measuring the P/Q through the static bypass switch, P_G and Q_G can be compared with the desired P^*_G and Q^*_G. The control laws PI_P and PI_Q, can be expressed as in the following:

$$\omega^*_{\mathrm{MG}} = k_{pP}\left(P^*_G - P_G\right) + k_{iP}\int\left(P^*_G - P_G\right)dt$$

$$E^*_{\mathrm{MG}} = k_{pQ}\left(Q^*_G - Q_G\right) + k_{iQ}\int\left(Q^*_G - Q_G\right)dt$$

with k_{pP} , k_{iP} , k_{pQ} , and k_{iQ} being the control parameters of the tertiary-control compensator. Here, ω^*_{MG} and E^*_{MG} are also saturated in case of being outside of the allowed limits. These variables are inner generated in island mode ($\omega^*_{MG} = \omega^*_i$ and $E^*_{MG} = E^*_{MG}$) by the secondary control. When the grid is present, the synchronization process can start, and ω^*_{MG} and E^*_{MG} can be equal to those measured in the grid. Thus, the frequency and amplitude references of the MG will be the frequency and amplitude of the mains grid. After the synchronization, these signals can be given by the tertiary control. Notice that, depending on the sign of P^*_G and Q^*_G, the active and reactive power flows can be exported or imported independently. This control loop can also be used to improve the power quality at the PCC. In order to achieve voltage-dip ride through, the MG must inject reactive power to the grid, thus achieving inner voltage stability. Islanding detection is also necessary to disconnect the MG from the grid and disconnect both the tertiary-control references as well as the integral terms of the reactive power PI controllers, to avoid voltage instabilities.

Simulation: grid connected DG

1) Initially, create an .mdl file.
2) Simulate a DG unit which consist of three phase VSC that are paralleled through an RL filter at PCC with a Synchronous Generator and exchanges active and reactive power. SG supplies an RL load.
3) Set the frequency and amplitude of the voltage of PCC by SG with help of Governor and AVR.
4) Control the DG based on primary level.
5) Evaluate performance of the controller in changing the RL load (increasing and decreasing PL and QL) based on voltage, frequency, active and reactive profiles of the DG and SG.
6) Discus on the results.

Simulation: Islanded Microgrid

1) Initially, create an .mdl file.
2) Simulate two DG unit which consist of three phase VSC that are paralleled through an LC filter at PCC and supply a variable RL load. (power sharing)
3) Control these DGs based on hierarchical control scheme. (Primary and secondary level are sufficient)
4) Evaluate performance of the inner, droop and secondary controllers in changing the RL load (increasing and decreasing P_L and Q_L) based on voltage, frequency, active and reactive profiles of the DGs.
5) Discus on the results.